Available online at www.sciencedirect.com
SCIENCE DIRECT
Journal of Magnetic Resonance 179 (2006) 85–91
JMR Journal of Magnetic Resonance
www.elsevier.com/locate/jmr

Synchronized detection of minute electrical currents with MRI using Lorentz effect imaging

Trong-Kha Truong *, Jennifer L. Wilbur, Allen W. Song

Brain Imaging and Analysis Center, Duke University, Durham, NC 27710, USA

Received 16 August 2005; revised 16 November 2005
Available online 15 December 2005

Abstract

The blood oxygenation level-dependent (BOLD) effect is the most commonly used contrast mechanism in functional magnetic resonance imaging (fMRI), due to its relatively high spatial resolution and sensitivity. However, the ability of BOLD fMRI to accurately localize neuronal activation in space and time is limited by the inherent hemodynamic modulation. There is hence a need to develop alternative MRI methods that can directly image neuroelectric activity, thereby achieving both a high temporal resolution and spatial specificity as compared to conventional BOLD fMRI. In this paper, we extend the Lorentz effect imaging technique, which can detect spatially incoherent yet temporally synchronized minute electrical activity in a strong magnetic field, and demonstrate its feasibility for imaging randomly oriented electrical currents on the order of microamperes with a temporal resolution on the order of milliseconds in gel phantoms. This constitutes a promising step towards its application to direct imaging of neuroelectric activity in vivo, which has the same order of current density and temporal synchrony.

Keywords: Lorentz effect imaging; Lorentz force; Electrical currents; Neuroelectric activity; Functional MRI

1. Introduction

Since its inception over a decade ago, functional magnetic resonance imaging (fMRI) has become a dominant non-invasive modality for neuroimaging research. The most commonly used contrast mechanism in fMRI is based on the blood oxygenation level-dependent (BOLD) effect [1–3], due to its relatively high spatial resolution and sensitivity. However, since BOLD fMRI is modulated by hemodynamics secondary to neuronal activity, its ability to accurately localize neuronal activation in space is limited by the complex vascular geometry of the brain, primarily because of signal contributions arising from the draining veins and their surroundings, which are distant from the sites of neuronal activity [4]. Furthermore, its ability to accurately localize neuronal activation in time is also limited by temporal delays and spatial dispersions resulting from the hemodynamic modulation [5]. This is also true in event-related fMRI studies, despite the high apparent temporal resolution [6]. On the other hand, techniques such as electroencephalography (EEG), magnetoencephalography (MEG), and event-related potential (ERP) recordings, which are more directly coupled to neuronal activity, benefit from an excellent temporal resolution on the order of milliseconds, but either have a poor spatial resolution or are extremely invasive. There is hence a need to develop an MRI technique that can directly image neuroelectric activity, thereby combining the high temporal resolution of electrical and magnetic recording methods with the non-invasiveness and high spatial resolution advantages inherent in MRI. Such a direct, real-time, and non-invasive neuroimaging technique would likely find broad applications in neurosciences.

Several groups have recently explored the feasibility of using MRI for direct imaging of neuronal activation, more specifically by attempting to detect the minute magnetic field changes induced either by electrical currents in phantoms

* Corresponding author. Fax: +1 919 681 7033.
E-mail address: truong@biac.duke.edu (T.-K. Truong).

1090-7807/$ - see front matter © 2005 Elsevier Inc. All rights reserved.
doi:10.1016/j.jmr.2005.11.012

[7–9] or by neuronal currents during evoked [10–13] or spontaneous [14] brain activity in human subjects. Despite some encouraging results, many issues remain controversial. For example, several simulations [9,14] and experimental [13] studies have shown that phase images are more sensitive to magnetic field changes induced by neuronal currents than magnitude images, yet others claim the opposite [11]. Furthermore, while many studies used gradient echo imaging [7,9–11,14], others have shown that spin echo imaging is preferable because it allows a better separation between the rapid magnetic field changes induced by neuronal currents and the slower ones due to the BOLD effect or motion [8–13]. More importantly, one study [12] specifically designed to separate the rapid (i.e., neuronal currents) from the slow (i.e., BOLD) signals while being highly sensitive to both has shown no significant effects from neuronal currents, thus suggesting that the positive results obtained in earlier studies [10,11] might in fact have been contaminated by the BOLD effect or other artifacts [12]. In another study, the detected effects could not be attributed with absolute certainty to neuronal currents, as high-frequency oscillations were unexpectedly found in vessels and cerebrospinal fluid [14]. All of these methods are intrinsically limited by the small magnitude of the magnetic field changes induced by neuronal activation. We therefore propose to use the Lorentz effect imaging (LEI) technique [15], which takes advantage of the strong static and gradient magnetic fields available on a modern MRI scanner, to detect minute electrical activity. In the present work, we extend this technique and demonstrate its feasibility for imaging electrical currents on the order of microamperes with a temporal resolution on the order of milliseconds in different gel phantoms.

2. Theory

2.1. Description of the LEI technique

The LEI technique relies on the well-known Lorentz effect, whereby a current-carrying conductor exposed to a magnetic field experiences a Lorentz force equal to the cross product of the current vector and the magnetic field. If the conductor is surrounded by an elastic medium, this force induces a displacement of the conductor and a compression of the elastic medium in adjacent regions, resulting in a spatially incoherent displacement of the spins in these regions. In the presence of a magnetic field gradient, these spins experience a loss of phase coherence, which in turn results in a destructive signal summation within a voxel similar to the transverse relaxation effect, causing an exponential signal decay.

Since a magnetic field gradient also induces a loss of phase coherence of the static spins, resulting in a global signal attenuation, balanced gradients (with positive and negative lobes of same amplitude and duration) are applied, so that the phase shifts experienced by the static spins are rephased,

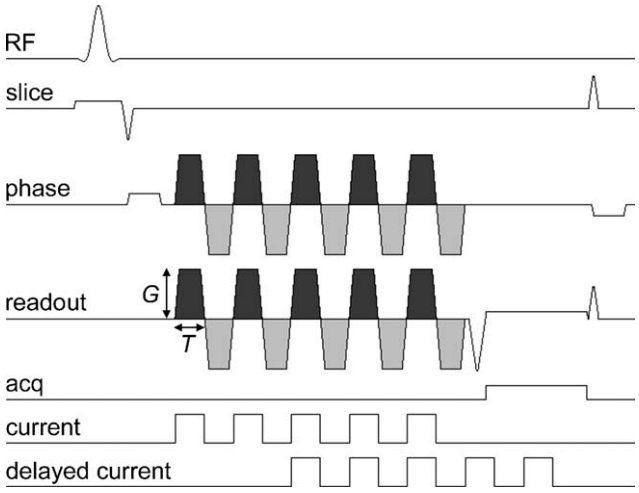

Fig. 1. Pulse sequence diagram. Gradient echo sequence with n (in this example, 5) cycles of oscillating magnetic field gradients (with positive and negative lobes of amplitude G and duration T, shown in dark and light gray) applied in the readout and phase encoding directions between excitation and data acquisition. The current is synchronized with the pulse sequence such that it turned on only during the positive lobes of the oscillating gradients. In the third study (bottom line), the current is delayed with respect to the oscillating gradients (in this example, by two cycles).

as in diffusion-weighted imaging. The current must then be synchronized with the pulse sequence such that it is turned on only during either the positive or the negative gradient lobe to preserve the phase shifts due to the Lorentz force-induced displacement. In this work, we incorporate a novel acquisition strategy whereby multiple cycles of such oscillating gradients synchronized with the current are used to drastically amplify the loss of phase coherence due to the incoherent displacement, and consequently significantly increase the sensitivity of the technique. More specifically, we use a gradient echo sequence with a series of oscillating gradients applied between excitation and data acquisition, and synchronized with the current such that it is turned on only during the positive lobes (Fig. 1).

2.2. Modelization of the signal loss

To get an insight into the contrast mechanism of the LEI technique, we consider a cylindrical current-carrying conductor oriented along the y axis, placed in a magnetic field oriented along the z axis, and surrounded by a homogeneous, isotropic, and linear elastic medium (Fig. 2A). The resulting Lorentz force, oriented along the x axis and proportional to the current and the magnetic field, induces a displacement of the conductor, leading to a spatially incoherent displacement of the surrounding elastic medium in the x direction. We assume that the deformation is elastic, i.e., the displacement is proportional to the applied force and inversely proportional to the Young's modulus of the elastic medium (Hooke's law). Furthermore, we assume that the conductor does not adhere to the elastic medium, so that it only induces a compression of the elastic medium

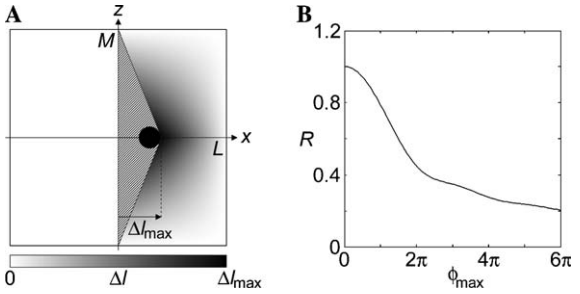

Fig. 2. Modelization of the signal loss. (A) A current-carrying conductor (black circle) orthogonal to the plane of the figure, placed in a magnetic field oriented along the z axis, and surrounded by an linear elastic medium, experiences a Lorentz force resulting in a spatially incoherent displacement $\Delta l(x,z)$ of the elastic medium in the x direction ranging between 0 and $\Delta l_{\max}$. It is assumed that there is no displacement in the $\{x<0\}$ region and that there is an empty space in the hatched region (see text). (B) Signal loss due to the Lorentz force-induced incoherent displacement in a voxel of dimensions $L\times M$ as a function of the maximum phase shift experienced by the elastic medium (Eq. (4)).

oscillating gradients (whose positive lobes are synchronized with the current) along the x axis is given by

$$\phi(x,z)=\gamma n\int_0^T G\Delta l(x,z)\,\mathrm{d}t\approx\gamma nGT\Delta l(x,z), \tag{3}$$

where G and T are the amplitude and duration of one gradient lobe respectively, and γ is the gyromagnetic ratio ($2\pi\times 42.57\times 10^6$ rad/T for protons). This phase shift is thus directly proportional to the displacement. To derive the right-hand side of Eq. (3), the displacement was assumed to occur over a time much shorter than T. If this were not the case, the resulting phase shift would be smaller.

The ratio of the signal intensity with and without Lorentz effect in a voxel of dimensions $L\times M$ can be computed by integrating the phase shift over the $\{0\leqslant x\leqslant L;\ 0\leqslant z\leqslant M\}$ region:

$$\begin{aligned}R&=\frac{\sqrt{\left[\int_0^M\int_{\Delta l_{\max}(M-z)/M}^{L}\rho'(z)\cos\phi(x,z)\,\mathrm{d}x\,\mathrm{d}z\right]^2+\left[\int_0^M\int_{\Delta l_{\max}(M-z)/M}^{L}\rho'(z)\sin\phi(x,z)\,\mathrm{d}x\,\mathrm{d}z\right]^2}}{\int_0^M\int_0^L\rho\,\mathrm{d}x\,\mathrm{d}z}\\&=\frac{1}{|\phi_{\max}|}\sqrt{\left(\int_0^{\phi_{\max}}\frac{\sin\alpha}{\alpha}\,\mathrm{d}\alpha\right)^2+\left(\int_0^{\phi_{\max}}\frac{1-\cos\alpha}{\alpha}\,\mathrm{d}\alpha\right)^2},\end{aligned} \tag{4}$$

in the direction of the displacement, but no dilation on the opposite side, thus leaving an empty space behind it. Because of the symmetry with respect to the z axis, we consider only the $\{z\geqslant 0\}$ region from now on. The maximum displacement $\Delta l_{\max}$ experienced by the elastic medium is equal to the displacement of the conductor and occurs at ($x=\Delta l_{\max}$, $z=0$). As a first order approximation, we assume that:

(1) there is no displacement in the $\{x\leqslant 0\}$, $\{x\geqslant L\}$, and $\{z\geqslant M\}$ regions;
(2) there is an empty space in the $\{0<x<\Delta l_{\max}(M-z)/M\}$ region (hatched in Fig. 2A);
(3) the displacement Δl at an arbitrary point (x,z) in the $\{\Delta l_{\max}(M-z)/M\leqslant x\leqslant L\}$ region decreases linearly from $\Delta l_{\max}$ to zero as follows:

$$\Delta l(x,z)=\frac{L-x}{L-\Delta l_{\max}\frac{M-z}{M}}\frac{M-z}{M}\Delta l_{\max}. \tag{1}$$

In this region, the spin density is therefore equal to

$$\rho'(z)=\rho\frac{L}{L-\Delta l_{\max}\frac{M-z}{M}}, \tag{2}$$

where ρ is the spin density in the absence of Lorentz force, and the phase shift obtained by applying n cycles of

where $\phi_{\max}=\phi(\Delta l_{\max})$. This expression thus represents the signal loss due to the Lorentz force-induced incoherent displacement, and is plotted as a function of $\phi_{\max}$ in Fig. 2B. Because of the complex nature of the compression of the elastic medium, the derivation of an analytical solution for a more general case is more difficult, and is beyond the scope of this paper. Nevertheless, the simplified model developed above does provide an insight into the signal loss mechanism of the LEI technique.

3. Methods

The following experimental studies were therefore carried out to validate this contrast mechanism, evaluate the sensitivity of the LEI technique for straight and randomly oriented currents, and demonstrate its high temporal resolution.

Two spherical phantoms (diameter 10 cm), hereafter referred to as phantoms A and B, were constructed. They consisted of carbon wires immersed in a gel made of 2.2% by weight gelatin. Phantom A contained a straight bundle of wires (overall diameter 500 μm), whereas phantom B contained 10 wires (diameter 100 μm) connected in parallel and oriented in random directions in three dimensions. For both phantoms, the wires were connected via shielded cables to a square wave pulse generator triggered by the positive lobes of the oscillating gradients, with a large resistor (>1 kΩ) connected in series to minimize any

current induced by the switching gradients that may contribute to the Lorentz effect.

Three studies were performed on a 4 T whole-body MRI scanner (General Electric Medical Systems, Milwaukee, WI) equipped with a high power gradient system (40 mT/m maximum amplitude, 150 T/m/s slew rate), using a shielded quadrature birdcage head coil and high order shimming. The studies were performed at high field strength to increase the sensitivity of the technique, since the magnitude of the Lorentz effect and the signal-to-noise ratio (SNR) both increase with field strength.

The acquisition parameters were optimized as follows. Eq. (3) shows that large values for n, G, and T should be used to amplify the loss of phase coherence and resulting signal decay due to the Lorentz force-induced displacement. However, the trade-off is an increased diffusion weighting, quantified by the following b-factor: $b = (2/3)n\gamma^2G^2T^3$ (for one gradient axis) [16], and resulting in a global signal attenuation. Since the phase shift is proportional to n, G, and T, whereas the b-factor is proportional to n, G^2, and T^3, it is preferable to use strong and short rather than weak and long oscillating gradients. Similarly, it is preferable to use a large number of short oscillating gradients rather than fewer long ones. Consequently, we chose $G = 40$ mT/m (the maximum achievable gradient amplitude) and $T = 2$ ms. Furthermore, another trade-off for using a large number of oscillating gradients is an increased echo time (TE), resulting in a global signal attenuation due to T_2^* relaxation. We experimentally determined that a value of $n = 15$, corresponding to a minimum TE of 71 ms, was optimal. This choice of parameters resulted in a b-factor of 9 s/mm^2, which causes a negligible signal attenuation due to diffusion weighting. Other parameters were as follows: repetition time 1000 ms, flip angle 70°, field-of-view 12 cm, matrix size 256×128, and slice thickness 5 mm.

The first study was conducted on phantom A to validate the newly developed technique and evaluate its sensitivity using the simplest geometry and a relatively thick wire (with respect to the voxel size). The phantom was positioned in the magnet with the wire orthogonal to the main magnetic field to maximize the Lorentz effect. Axial images were acquired with oscillating gradients applied in the direction orthogonal to both the wire and the main magnetic field, since the Lorentz force-induced displacement occurs in that direction. Current intensities of 0, 5, 10, 20, 50, 100, 200, and 500 μA were applied, thus covering the range of values found in biological systems. Five averages were used for currents up to 20 μA to increase the SNR.

The second study was conducted on phantom B to demonstrate the feasibility of the LEI technique to detect currents flowing in multiple directions with a more complex geometry. All parameters were identical to those used in the first study, except that oscillating gradients were applied along both directions orthogonal to the main magnetic field. The LEI technique can detect displacements occurring in multiple directions whether oscillating gradients are applied along only one axis or both axes orthogonal to the main magnetic field. In either case, it is most (respectively least) sensitive to displacements occurring in a direction parallel (respectively orthogonal) to the direction of the largest gradient. However, this largest gradient is a factor $\sqrt{2}$ larger, and consequently the overall sensitivity is higher, when oscillating gradients are applied along both axes rather than only one axis (assuming they have the same amplitude).

The third study was designed for two purposes: first, to demonstrate that the observed signal loss is due to the intravoxel dephasing resulting from the spatially incoherent displacement of the gel rather than to the displacement of the wire itself (as the wire does not generate any MR signal), and second, to demonstrate the high temporal resolution of the LEI technique. In this study, the current intensity was fixed at 500 μA and the current was delayed with respect to the positive lobes of the oscillating gradients by 0–15 cycles, resulting in an overlap of 15–0 cycles between the two, respectively (Fig. 1, bottom line). As such, the Lorentz force-induced displacement was kept constant, while the loss of phase coherence and resulting signal decay due to the incoherent displacement was varied. The study was conducted on phantom A with all other parameters identical to those used in the first study. The image acquired with no overlap between the current and the oscillating gradients served as the reference and was therefore acquired using five averages to increase the SNR.

4. Results

4.1. Current density dependence for a straight current

The results of the first study are shown in Fig. 3. As expected, the central signal dip observed on the image acquired without current (Fig. 3A), which is due to the presence of the wire, becomes progressively larger and wider with increasing current intensities, as can be seen more clearly on the difference images (Fig. 3B). This signal loss, caused by the intravoxel dephasing due to the Lorentz force-induced incoherent displacement, occurs only on one side of the wire, as shown on the plot of the average signal intensity profiles across the wire (Fig. 3C). Similar results are obtained when the direction of the current is reversed, except that the displacement occurs in the opposite direction. The widening can reach up to 750 μm (full width at half maximum) for a current intensity of 500 μA, with a corresponding maximal signal loss of 25%. Yet, currents as low as 5 μA can still be detected.

The wire does not adhere to the gel and does therefore not exert any force on the gel on the side opposite to its displacement. Consequently, the displacement of the wire only induces a compression of the gel in the direction of the displacement, but no dilation on the opposite side, which explains why a signal loss is observed only on one side of the wire, namely towards the bottom of the image, as

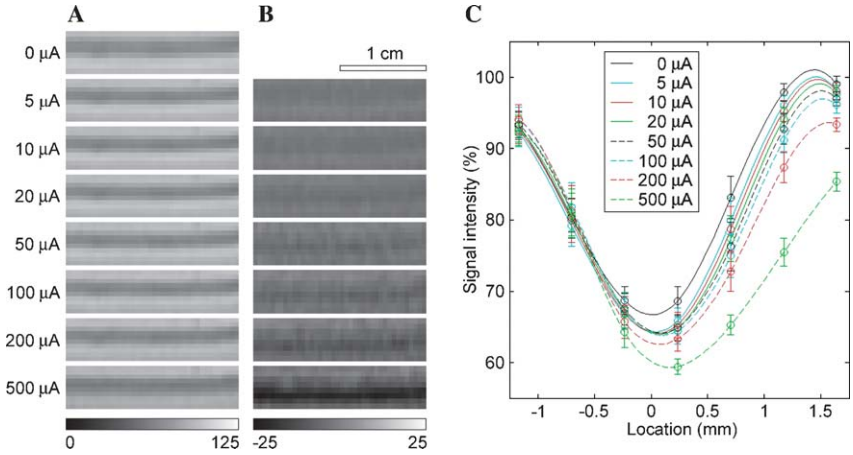

Fig. 3. Current density dependence for a straight current. (A) Images of a selected region of phantom A containing the wire acquired with different current intensities. (B) Corresponding difference images with the image acquired without current. (C) Signal intensity profiles across the wire averaged over the section shown in (A) and (B) for the different current intensities. The lines are computed using cubic spline interpolation. The signal intensity in (A)–(C) is expressed in % of the maximum signal in the image acquired without current.

expected for a current flowing from the right to the left and a magnetic field going into the plane of the image. Nevertheless, it is important to note that even if this were not the case (e.g., for a neuron surrounded by tissue), a dilation of the elastic medium on the side opposite to the direction of the displacement would induce a spatially incoherent displacement and a loss of phase coherence similar to those induced by the compression of the elastic medium on the opposite side, thus resulting in a signal loss on both sides and making the technique even more sensitive.

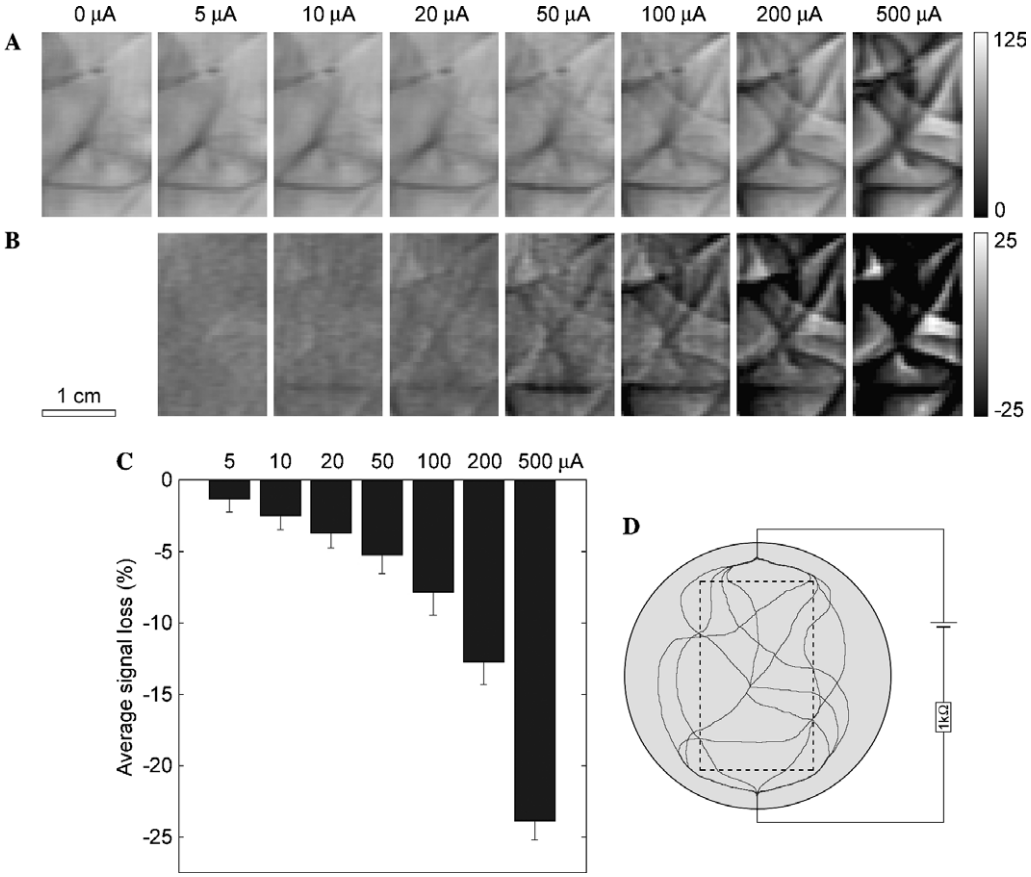

Fig. 4. Current density dependence for randomly oriented currents. (A) Images of a selected region of phantom B acquired with different current intensities. (B) Corresponding difference images with the image acquired without current. (C) Signal loss averaged over the region shown in (A) and (B) for the different current intensities. The signal intensity in (A)–(C) is expressed in % of the maximum signal in the image acquired without current. (D) Schematic illustration of the phantom. The dashed rectangle corresponds to the region shown in (A) and (B).

4.2. Current density dependence for randomly oriented currents

The results of the second study are shown in Fig. 4 and demonstrate that the LEI technique can detect currents flowing in multiple directions. As for the straight wire in the first study, the signal losses correspond to the wire locations (Fig. 4D) and become more pronounced with increasing current intensities, which can be clearly seen on both the original images (Fig. 4A) and the difference images (Fig. 4B). To better assess the overall effect, the signal loss was averaged over the whole region shown in Figs. 4A and B, and is plotted in Fig. 4C for the different current intensities. The resulting absolute values are not meaningful since they depend on the current density within the region over which the average was computed. Nevertheless, the plot clearly shows that the average signal loss progressively increases with the current intensity. Currents as low as 5 μA can still be detected, although only in some areas, depending on the local current distribution. For example, the segments of wire that were not orthogonal to the main magnetic field experienced a smaller Lorentz force and therefore a smaller signal loss.

4.3. Dependence on the overlap between the current and the oscillating gradients

The results of the third study are shown in Fig. 5. As expected, the signal loss progressively increases with the amount of overlap between the current and the positive lobes of the oscillating gradients, which can be clearly seen on both the difference images (Fig. 5B) and the plot of the average signal loss (Fig. 5C). The small overall signal increase observed for one cycle of overlap is due to the very low contrast-to-noise ratio for that condition.

These results first demonstrate that the observed signal loss is due to the intravoxel dephasing resulting from the spatially incoherent displacement of the gel rather than to the displacement of the wire itself, since the amount of dephasing increased with the overlap between the current and the positive lobes of the oscillating gradients, while the displacement of the wire remained constant in this study. A similar conclusion can be reached by acquiring different images of the phantom using a fixed current intensity and varying the amplitude of the oscillating gradients.

Furthermore, these results clearly show that the LEI technique is sensitive to temporal offsets between the current and the oscillating gradients as small as 4 ms, thus demonstrating that it can achieve a temporal resolution on the order of milliseconds, which represents a substantial improvement as compared to conventional BOLD fMRI. This limit could potentially be further improved by increasing the sensitivity of the technique.

5. Discussion and conclusions

The results presented in this paper clearly demonstrate the feasibility of the LEI technique for imaging randomly oriented electrical currents on the order of microamperes with a temporal resolution on the order of milliseconds.

The fact that a signal loss can only be observed on one side of the wire in Fig. 3C shows that it is predominantly due to the Lorentz force-induced displacement rather than to magnetic field changes induced by the current, which would otherwise result in a signal loss on both sides of the wire. To further validate this signal loss mechanism with a more complex geometry, we acquired images of phantom B using current intensities of 0 and 500 μA and other parameters otherwise identical, except that the amplitude of the oscillating gradients was set to zero. No signal loss could be detected between the two conditions, which confirms that the magnitude images acquired with the LEI technique are not significantly affected by magnetic field changes induced by the current, but also shows that they are not affected by eddy currents either. This observation is consistent with the studies demonstrating that magnitude images are less sensitive to magnetic field changes

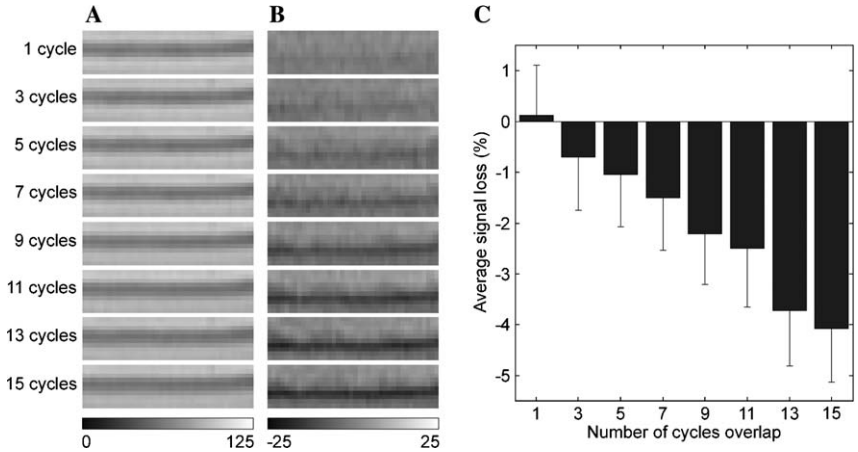

Fig. 5. Dependence on the overlap between the current and the oscillating gradients. (A) Images of a selected region of phantom A containing the wire acquired with a 500 μA current and different amounts of overlap between the current and the positive lobes of the oscillating gradients. (B) Corresponding difference images with the image acquired without overlap. (C) Signal loss averaged over the region shown in (A) and (B) for the different amounts of overlap. The signal intensity in (A)–(C) is expressed in % of the maximum signal in the image acquired without overlap.

induced by typical neuronal currents than phase images (e.g., [14]).

By applying successive cycles of oscillating gradients and using optimized parameters, the sensitivity of the LEI technique was substantially improved as compared to a previous study [15], despite the lower field strength and weaker oscillating gradients used in the present work. A current of 5 μA is comparable to the smallest detectable currents reported in previous phantom studies based on phase imaging, namely 10 μA [8] and 1.5 μA [9] (both at 3 T). The sensitivity of the LEI technique can obviously be improved by using a larger number of averages. Moreover, unlike for methods relying on magnetic field changes induced by the current, which are independent of the main magnetic field strength, the sensitivity of the LEI technique can be further increased by using a higher field strength (more specifically, beyond the improvement due to the increase in SNR alone) and/or stronger oscillating gradients, as such advances in hardware become increasingly more available on modern MRI scanners.

Assuming that $n = 15$, $G = 40$ mT/m, and $T = 2$ ms, as used in this work, the model shows that a signal loss of 5%, which is on the order of magnitude of what is measured, corresponds to a displacement $\Delta l_{\max}$ of about 5 μm (Eqs. (3) and (4)). This gives an indication of what range of displacements the LEI technique is sensitive to for the oscillating gradients parameters used here. However, it is important to note that the exact magnitude of the displacement is not relevant, since for the same displacement the sensitivity can be arbitrarily enhanced by using stronger oscillating gradients, which is one of the main advantages of this technique.

The results obtained in this work with the LEI technique constitute a promising step towards its application to direct imaging of neuroelectric activity in vivo, which has the same order of current density and temporal synchrony as the electrical currents used here. Indeed, the current generated by a single neuron is on the order of nanoamperes, depending on its diameter, so that the synchronized activity of a functional cortical unit, typically consisting of 10^4–10^5 neurons/mm^2, can generate a current density on the order of tens of μA/mm^2, which is similar to what was detected in our studies. Nevertheless, such an application to in vivo studies remains experimentally challenging. Synchronized confounding factors, such as functional signals reflecting BOLD, cerebral blood volume, and cerebral blood flow changes, as well as physiological noise, can dominate the detected signal. Therefore, a careful design of the experimental paradigm is required to separate these slow effects from the rapid effects due to neuroelectric activity. In addition, a very accurate synchronization between the stimulation and image acquisition is mandatory for this application. Such efforts to implement the LEI technique for direct imaging of neuroelectric activity in vivo are currently underway. With the high spatial resolution inherent in MRI, this direct, real-time, and non-invasive neuroimaging technique would achieve both a high temporal resolution and spatial specificity as compared to conventional BOLD fMRI, and could thus possibly track neural electrical conduction. As such, it could potentially find broad applications in neurosciences.

Acknowledgments

We thank Dr. Todd Harshbarger, Hua Guo, and Bin Chen for helpful comments on the manuscript. This work was supported by Grants NS 50329 and NS 41328 from the National Institutes of Health.

References

[1] K.K. Kwong, J.W. Belliveau, D.A. Chesler, I.E. Goldberg, R.M. Weisskoff, B.P. Poncelet, D.N. Kennedy, B.E. Hoppel, M.S. Cohen, R. Turner, H.-M. Cheng, T.J. Brady, B.R. Rosen, Dynamic magnetic resonance imaging of human brain activity during primary sensory stimulation, Proc. Natl. Acad. Sci. USA 89 (1992) 5675–5679.
[2] P.A. Bandettini, E.C. Wong, R.S. Hinks, R.S. Tikofski, J.S. Hyde, Time course EPI of human brain function during task activation, Magn. Reson. Med. 25 (1992) 390–397.
[3] S. Ogawa, D.W. Tank, R. Menon, J.M. Ellermann, S.G. Kim, H. Merkle, K. Ugurbil, Intrinsic signal changes accompanying sensory stimulation: functional brain mapping with magnetic resonance imaging, Proc. Natl. Acad. Sci. USA 89 (1992) 5951–5955.
[4] S. Lai, A.L. Hopkins, E.M. Haacke, D. Li, B.A. Wasserman, P. Buckley, L. Friedman, H. Meltzer, P. Hedera, R. Friedland, Identification of vascular structures as a major source of signal contrast in high resolution 2D and 3D functional activation imaging of the motor cortex at 1.5 T: preliminary results, Magn. Reson. Med. 30 (1993) 387–392.
[5] S.G. Kim, W. Richter, K. Ugurbil, Limitations of temporal resolution in functional MRI, Magn. Reson. Med. 37 (1997) 631–636.
[6] R.L. Buckner, Event-related fMRI and the hemodynamic response, Hum. Brain Mapp. 6 (1998) 373–377.
[7] J. Bodurka, A. Jesmanowicz, J.S. Hyde, H. Xu, L. Estkowski, S.J. Li, Current-induced magnetic resonance phase imaging, J. Magn. Reson. 137 (1999) 265–271.
[8] J. Bodurka, P.A. Bandettini, Toward direct mapping of neuronal activity: MRI detection of ultraweak, transient magnetic fields changes, Magn. Reson. Med. 47 (2002) 1052–1058.
[9] D. Konn, P. Gowland, R. Bowtell, MRI detection of weak magnetic fields due to an extended current dipole in a conducting sphere: A model for direct detection of neuronal currents in the brain, Magn. Reson. Med. 50 (2003) 40–49.
[10] H. Kamei, K. Iramina, K. Yoshikawa, S. Ueno, Neuronal current distribution imaging using magnetic resonance, IEEE Trans. Magn. 35 (1999) 4109–4111.
[11] J. Xiong, P.T. Fox, J.H. Gao, Directly mapping magnetic field effects of neuronal activity by magnetic resonance imaging, Hum. Brain Mapp. 20 (2003) 41–49.
[12] R. Chu, J.A. de Zwart, P. van Gelderen, M. Fukunaga, P. Kellman, T. Holroyd, J.H. Duyn, Hunting for neuronal currents: absence of rapid MRI signal changes during visual-evoked response, Neuroimage 23 (2004) 1059–1067.
[13] M. Bianciardi, F. Di Russo, T. Aprile, B. Maraviglia, G.E. Hagberg, Combination of BOLD-fMRI and VEP recordings for spin-echo MRI detection of primary magnetic effects caused by neuronal currents, Magn. Reson. Imag. 22 (2004) 1429–1440.
[14] D. Konn, S. Leach, P. Gowland, R. Bowtell, Initial attempts at directly detecting alpha wave activity in the brain using MRI, Magn. Reson. Imag. 22 (2004) 1413–1427.
[15] A.W. Song, A.M. Takahashi, Lorentz effect imaging, Magn. Reson. Imag. 19 (2001) 763–767.
[16] E.O. Stejskal, J.E. Tanner, Spin diffusion measurements: spin echoes in the presence of a time-dependent field gradient, J. Chem. Phys. 42 (1965) 288–292.